CORRECTION OF TRAVELTIMES AND ATTRIBUTES

Nils-Alexander Müller

email: *alex.mueller@gpi.uni-karlsruhe.de*
keywords: *CRS, attributes, spread-length bias*

ABSTRACT

When performing coherence analyses for the purpose of stacking and attribute determination, systematic errors may be introduced into the results. This is due to traveltime approximations in the coherence operators which are not sufficient for the description of the given data. In this paper, we describe how these errors can be corrected for using multiple coherence analyses with different configurations. The method is especially designed for the 2-D Common-Reflection-Surface stacking operator. However, a generalization of the technique to other operators is straightforward.

INTRODUCTION

Producing stack and attribute sections from pre-stack data by means of the Common-Reflection-Surface (CRS) stack (see, e.g., Höcht et al., 1999) assumes that reflection events can be described by a second-order approximation of the traveltime. A common way to perform the CRS stack is to apply a coherence analysis. Doing so, the second order assumption also enters into the respective coherence criterion (in general the semblance operator). As the coherence analysis yields "best fit" quantities, for non-second-order reflection events the actually obtained parameters A_S^K differ from the searched for first and second order attributes A_0^K (this misfit is often called "spread-length bias"). In the same way the estimated "best fit" zero-offset (ZO) traveltimes t_S (and thus the ZO stack) do, in general, not coincide with the real ZO-traveltimes t_{ZO} (see, e.g., Hubral and Krey, 1980; Shah and Levin, 1973).

In order to correct for these errors we introduce a new attribute α_T ("timedip") which is related to a data volume obtained from multiple CMP stacks and coherence analyses with different apertures (the "CMP-aperture" (CMPA) volume). Assuming a linear relationship between spread-length bias and search aperture for attributes and traveltimes this parameter is then used to extrapolate corrected CRS attributes as well as a time-corrected ZO stack section. As will be show for the example of tomography with subsequent depth migration, these corrected quantities yield better results in applications based on CRS attributes and traveltimes than the conventional approach without corrections.

THE COMMON-REFLECTION-SURFACE STACK

The aim of performing a 2-D CRS stack is to obtain a CRS stacked ZO section as well as the kinematic wavefield attributes of the CRS stack, namely the radii of curvature of the Normal-Incidence-Point (NIP) and normal (N) wave (R_{NIP} and R_{N}) and the emergence angle α of the ZO ray at the surface. The corresponding hyperbolic stacking operator or traveltime approximation reads

$$\begin{aligned} t_{\text{hyp}}^2 &= \left(t_0 + \frac{2\sin(\alpha)}{v_0}\Delta x_m\right)^2 + \frac{2t_0\cos^2(\alpha)}{v_0}\left(\frac{\Delta x_m^2}{R_{\text{N}}} + \frac{h^2}{R_{\text{NIP}}}\right) \\ &= \left(t_0 + 2p\Delta x_m\right)^2 + N\Delta x_m^2 + Mh^2\,, \end{aligned} \tag{1}$$

with v_0 being the near-surface velocity, Δx_m the midpoint displacement, h the half-offset in the CMP gathers, and t_0 the ZO traveltime under consideration.

In order to perform the CRS stack the three attributes $M = 2t_0 \cos^2\alpha/(v_0 R_{\text{NIP}})$, $p = \sin\alpha/v_0$, and $N = 2t_0 \cos^2\alpha/(v_0 R_{\text{N}})$, have to be determined. In practice, the search for these quantities is performed in three subsequent steps (see, e.g. Mann, 2002): a first search in the CMP domain ($\Delta x_m = 0$) yields M and a CMP stacked ZO section. In the latter ZO section (defined by $h = 0$) a linear search for p (assuming $N = 0$) followed by a hyperbolic search for N are applied. Knowing the three quantities M, N, and p , the CRS stacking operator (1) can finally be applied to the pre-stack data in order to obtain the CRS stacked ZO section. In addition the kinematic wavefield attributes R_{NIP}, R_{N}, and α can be evaluated.

The three stacking operators related to the three different searches read

$$t^2_{\text{hyp,CMP}} = t_0^2 + Mh^2 \,, \tag{2}$$

$$t_{\text{hyp,LZO}} = t_0 + 2p\Delta x_m \,, \tag{3}$$

$$t^2_{\text{hyp,HZO}} = (t_0 + 2p\Delta x_m)^2 + N\Delta x_m^2 \,. \tag{4}$$

As can be seen in equations (2)-(4) the searched for parameters are always related to the term with lowest possible, non-constant order, i.e., M constitutes the second order term in equation (2) (the first order term vanishes in the CMP configuration), p the first order term in equation (3), and N the second order term in equation (4) (assuming p is known).[1]

CORRECT AND "BEST FIT" ATTRIBUTES

In conventional implementations of the CRS stack the search for the three attributes is done by means of a coherence analysis. As mentioned in the introduction this yields "best fit" attributes M_S, N_S, and p_S and traveltimes t_S which are, in general, different from the correct attributes M, N, and p and traveltime t_{ZO}. Besides e.g., coherence band width, wavelet type, and trace distribution, the amount of misfit (spread length bias) between "best fit" and correct wavefield attributes and traveltimes depends on the aperture ξ used in the coherence analysis. If all quantities except for this aperture are kept constant, the relation between "best fit" and correct values for a reflection event with ZO traveltime t_{ZO} may be written as

$$t_S(\xi) = t_{\text{ZO}} + f(\xi) \,, \tag{5}$$

$$A^K_S(\xi, t_S) = A^K_{t_{\text{ZO}}} + g^K_{t_{\text{ZO}}}(\xi) \,, \tag{6}$$

with $A^K_S(\xi, t_S)$ being one of the "best fit" and $A^K_{t_{\text{ZO}}}$ the respective correct attributes (indexed by the superscript K). Functions $f(\xi)$ and $g^K_{t_{\text{ZO}}}(\xi)$ denote unknown, aperture dependent functions describing the spread-length bias between "best fit" and correct values. In the following two properties are assumed to be valid for $f(\xi)$ and $g^K_{t_{\text{ZO}}}(\xi)$, respectively: their first derivatives, i.e., $f'(\xi)$ and ${g^K_{t_{\text{ZO}}}}'(\xi)$, exist, and the misfit vanishes for zero-aperture, i.e., $f(0) = 0$ and $g^K_{t_{\text{ZO}}}(0) = 0$. The first property states that the seismic data does not contain sudden changes or breaks, the second one requires the coherence analysis to tend toward the correct attributes when using small apertures. This can be justified when considering that lower order terms dominate a series at small deviations from the expansion point. As mentioned before these lower order terms are exactly the searched for attributes, so they will dominate the coherence analysis and, thus, the results for $\xi \to 0$.

In general, the functions $f(\xi)$ and $g^K_{t_{\text{ZO}}}(\xi)$ are not known. For that reason they are expanded into a Mac-Laurin series up to first order, i.e., only the linear term is retained:

$$f(\xi) \approx a \cdot \xi \;\text{ with }\; a = f'(0) \,, \tag{7}$$

$$g^K_{t_{\text{ZO}}}(\xi) \approx b^K \cdot \xi \;\text{ with }\; b = {g^K_{t_{\text{ZO}}}}'(0) \,. \tag{8}$$

Inserting equations (7) and (8) into equations (5) and (6) a linearized approximation for the relationship between correct and "best fit" attributes is achieved:

$$t_S(\xi) \approx t_{\text{ZO}} + a \cdot \xi \quad \Leftrightarrow \quad t_{\text{ZO}} \approx t_s(\xi) - a \cdot \xi \,, \tag{9}$$

$$A^K_S(\xi, t_S) \approx A^K_{t_{\text{ZO}}} + b^K \cdot \xi \quad \Leftrightarrow \quad A^K_{t_{\text{ZO}}} \approx A^K_S(\xi, t_S) - b^K \cdot \xi \,. \tag{10}$$

Equations (9) and (10) state that with the knowledge of a and b^K, respectively, the "best fit" quantities can be approximately computed from correct attributes and vice versa.

[1] Low order terms approximate the real function best at small distances from the expansion point. For that reason equations (2)-(4) are also called "small-spread approximations".

CORRECTION OF MISFITS

In order to correct "best fit" attributes, the unknown quantities a and b^K have to be determined from the available data in some way. Knowing these parameters, corrected CRS attributes and traveltimes can be calculated by evaluating equations (9) and (10) for zero-aperture, i.e., $\xi = 0$. In this paper we will discuss techniques for the determination of a and b^K and the subsequent correction of "best fit" attributes by means of the CMP search of the CRS stack, i.e., the determination of M and the respective CMP stacked ZO section. Similar corrections can be obtained for other operations based on coherence analysis, e.g., in context with the CRS stack the searches for p and N. However, the CMP search has, due to its dominant character in the CRS processing chain, the largest impact on the final results.

Determination of a and $t_{\mathbf{ZO}}$

The determination of a and the correction of the traveltime t_S to t_{ZO} starts with the application of a series of CMP searches with different search apertures ξ. A new pseudo pre-stack data volume $\mathbf{T}(x, t_S, \xi)$ is then constructed from the CMP stacked ZO sections. This "CMP-aperture" (CMPA) volume consists of the different CMP stacked sections parameterized by trace locations x and traveltimes t_S and the search aperture ξ as third dimension. In this volume, a coherence analysis related to the searched-for zero-aperture plane $\mathbf{T}(x, t_S \equiv t_{\mathrm{ZO}}, \xi = 0)$ is performed. The corresponding traveltime approximation is based on equation (9) and reads

$$t_S = t_{\mathrm{ZO}} + \frac{\sin(\alpha_T)}{v_0} \cdot \xi \; . \tag{11}$$

Here, parameter a in equation (9) has been replaced by the term $\sin(\alpha_T)/v_0$ with the "timedip" α_T in order to obtain a more vivid representation of the process.

Outcome of this coherence analysis are a timedip section and, performing a subsequent stack using this section, a stacked ZO section with corrected traveltimes t_{ZO}.

Determination of b^K and $A^K_{t_{\mathbf{ZO}}}$

Similar to the determination of a the determination of b^K starts with the construction of a new CMPA volume: the different M_S sections obtained from the CMP searches form the volume $\mathbf{A}(x, t_S, \xi)$. Also, the output section is defined by the zero-aperture plane $\mathbf{A}(x, t_S \equiv t_{\mathrm{ZO}}, \xi = 0)$. For each sample j in this plane, the previously obtained timedip section together with stacking operator (11) define linear trajectories in $\mathbf{A}(\mathbf{x}, \mathbf{t_S}, \xi)$ along which sets L_j of data points $(M_S(\xi), \xi)$ are extracted, i.e., the timedip section is used to follow the reflection events in ξ-direction. A linear regression is then applied on each L_j; the regression coefficients coincide with b^K as well as the corrected attribute $A^K_{t_{\mathrm{ZO}}}$, which is in this case the searched for M. Thus, the result of this process is a section with the corrected M.

ZO processing and CRS stack

A consequence of the three successive CRS processing steps is, that the CMP stacked ZO section enters directly into the two ZO searches for p and N. As this section contains incorrectly positioned reflection events, errors will be introduced to the attributes p and N, too. This can be avoided if the corrected ZO section from the determination of a is used for ZO processing instead.

The final CRS stack itself can not be performed with the corrected attributes $A^K_{t_{\mathrm{ZO}}}$. In contrast to "best fit" attributes A^K_S they are not designed for the purpose of imaging and they will likely produce stacked sections with much more artifacts and noise. However, applications based on attributes should show better results.

SYNTHETIC DATA EXAMPLE

The proposed strategy has been applied to a synthetic dataset modelled for the velocity model shown in Figure 1(a). A forward modelled ZO section can be found in Figure 1(b).

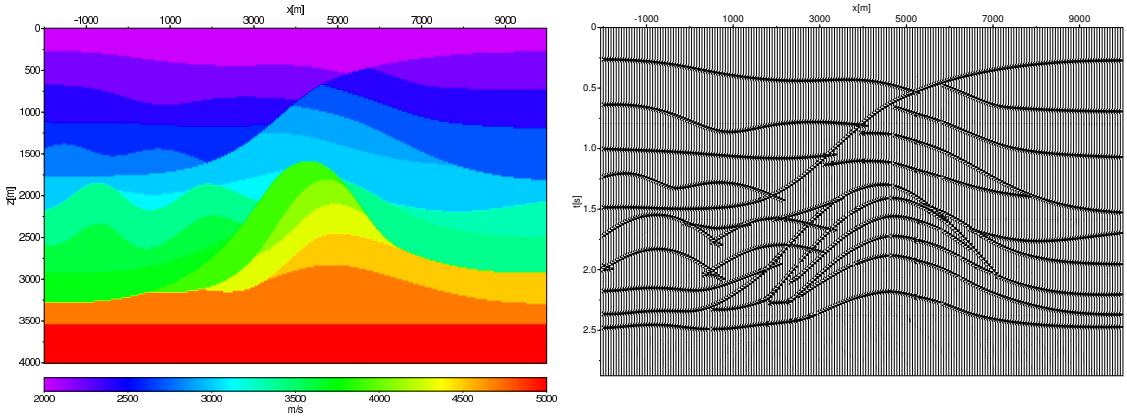

(a) Velocity model. **(b)** ZO section.

Figure 1: Velocity model (left) and forward modelled ZO section of the synthetic dataset.

Multiple CMP searches

As described above, the first step is to perform multiple CMP searches with different apertures ξ. The chosen apertures lay in the range $\xi = [1000\text{ m}, 3200\text{ m}]$ with a step size of 100 m, i.e., 23 different CMP searches were realized. Figure 2 shows the traveltime misfit between the forward modelled and CMP stacked section ($\xi = 3200$ m) for a subset of the complete ZO section. As can be seen, the maximum traveltime deviation is about $1/4$ wavelet length.

From the results of the 23 CMP searches the CMPA stack and M_S volumes shown in Figures 3(a) and 3(b) were constructed.

Traveltime and attribute corrections

The CMPA stack volume was now used by a coherence analysis with equation (11) as traveltime approximation. The resulting timedip section (shown in Figure 4(a)) demonstrates that the most significant corrections have to be applied in the region of the central dome where α_T, and, thus, the aperture dependent traveltime misfit, is largest. A subset of the corresponding corrected stack section is shown in Figure 6. As can be seen the misfit in traveltimes has been greatly reduced compared to the large aperture section depicted in Figure 2. By means of the CMPA M_S volume and the timedip section the M_S were finally corrected to the searched for zero aperture M (see Figure 4(b)) by a linear regression. Figure 5(a) shows that the percentile difference between the original attribute at aperture $\xi = 3200$ m and the corrected one reaches up to 50%.

The modified shape of the reflection events in the corrected CMP stacked section is also relevant for the two following searches for p and N. Figure 5(b) shows the difference in the emergence angles α after searches in the corrected and a large aperture ($\xi = 3200$ m) section. This figure demonstrates that even for such small traveltime misfits as $1/4$ wavelet length (which may actually sum up to $1/2$ wavelet length of total misfit if considering more than one trace), attributes may vary significantly if they require correct stacked sections for their determination.

Quality of the corrected attributes and traveltimes

The quality of the corrected attributes has been tested by a NIP wave tomography (see, e.g., Duveneck, 2004) followed by a pre-stack depth migration. If the attributes and traveltimes were correctly extrapolated to zero-aperture, Common-Image-Gathers (CIG) from pre-stack depth migration should generally become flatter. Also, the depth locations of the reflections events should be improved.

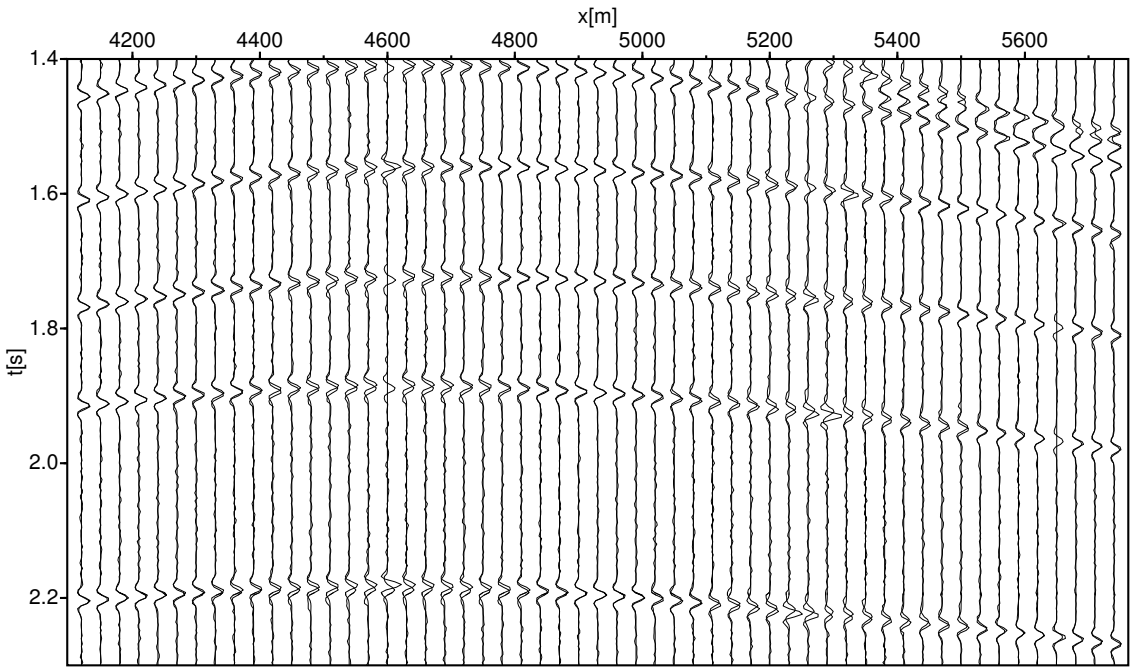

Figure 2: Misfit between forward modelled and CMP stacked ($\xi = 3200$ m) ZO sections in the center of the synthetic dataset.

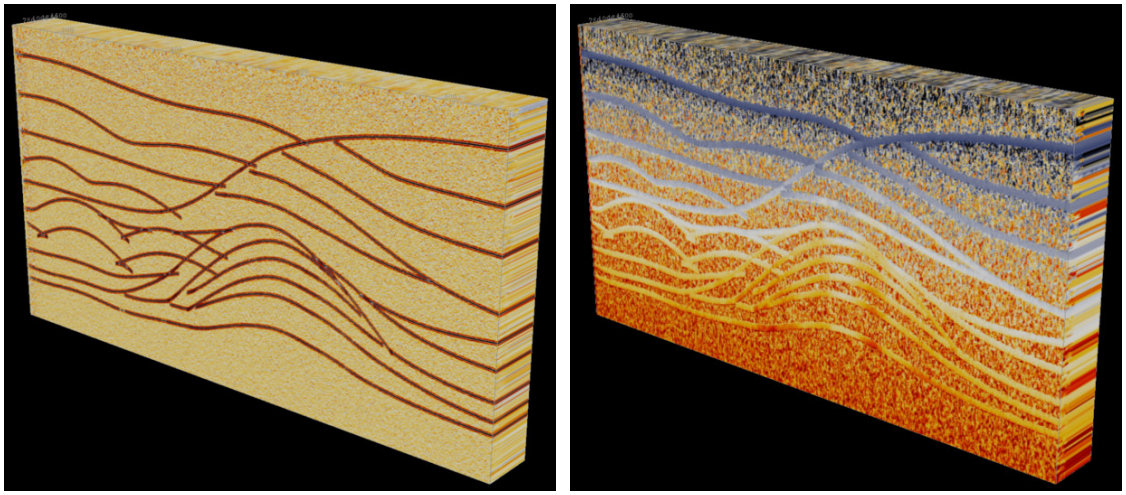

(a) CMP volume.

(b) M volume.

Figure 3: CMPA volumes obtained by multiple CMP searches. The left side shows a volume of CMP stacks, the right side a volume of M_S sections.

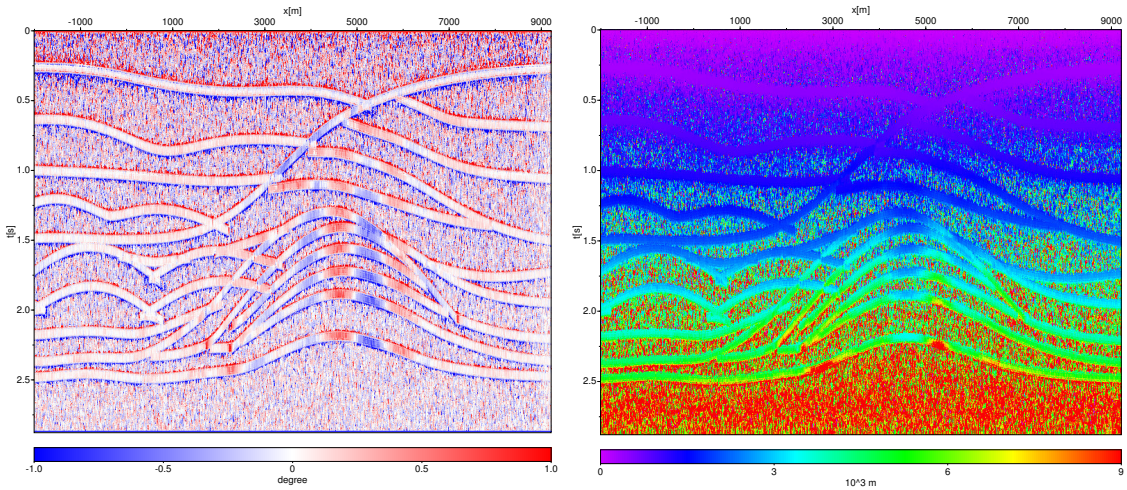

(a) Timedip α_T section **(b)** M section

Figure 4: Timedip α_T (left) and M (right) sections obtained from the CMPA stack and M_S volumes.

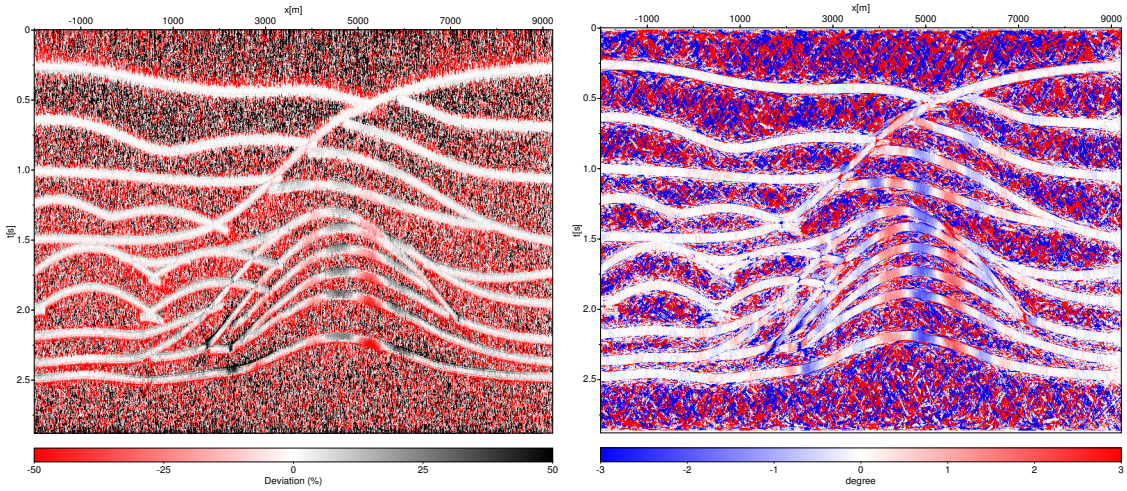

(a) Change of M **(b)** Change of α

Figure 5: Left: percentile change of $M_S(\xi = 3200\,\mathrm{m})$ after correction to M. Right: differences in the emergence angle α after searches in corrected and $\xi = 3200$ m stack sections.

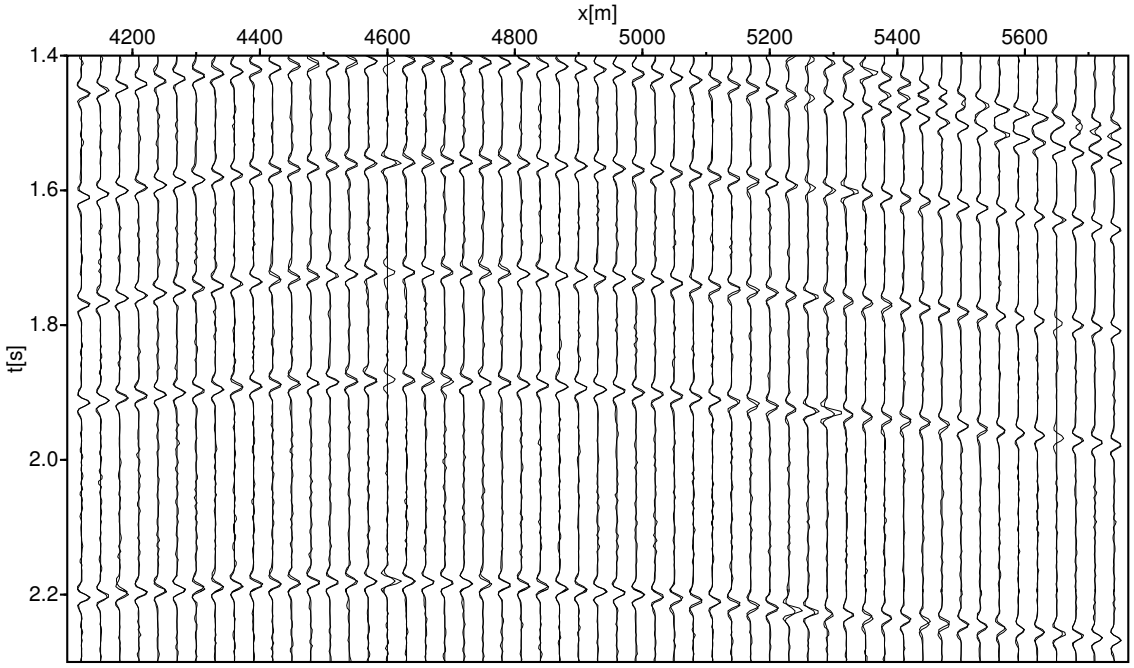

Figure 6: Misfit between forward modelled and corrected ($\xi = 0$ m) ZO sections in the center of the synthetic dataset.

For comparison, tomography and migration have been performed on the corrected data as well as on conventional data with search aperture $\xi = 3200$ m.

NIP wave tomography The input data for NIP wave tomography was automatically picked from the attributes obtained from conventional processing and from the correction. Each of the datasets consisted of approximately 2130 picks. Tomography was performed on a velocity model with a knot-spacing of 300 m in x-direction and 200 m in z-direction. The processing was performed with equal setups for both datasets.

Figure 7(a) shows the velocity model obtained from the dataset with corrected attributes, Figure 7(b) the velocity difference model of both datasets. Although there are velocity differences of up to 250 m/s, both velocity models explain the kinematics and, thus, the depth locations of the picks relatively well (see Figures 8(a) and 8(b)). However, having a closer look one can see that inside and at the flanks of the dome the corrected dataset provides a better coincidence with the original model.

Pre-stack depth migration The final test for the quality of the corrected attributes is a pre-stack depth migration. For both tomographic velocity models the migration was performed with offsets up to 2000 m. The results are depicted in Figures 9(a) and 9(b). It is clearly visible that almost everywhere the Common-Image-Gathers related to the corrected attributes show less moveout than their counterparts obtained by conventional processing. Furthermore the model structure is, as already mentioned, closer to the original model. This means, that the corrected attributes and traveltimes do in fact provide much better results than "best fit" quantities.

CONCLUSIONS

In this paper, a technique for the minimization of the spread-length bias between coherence based "best fit" and analytical attributes and traveltimes has been presented. The method is based on CMPA volumes obtained by multiple coherence analyses with different search apertures. Using CMPA stack volumes, the "best fit" traveltimes are corrected by an additional coherence analysis related to an attribute α_T which

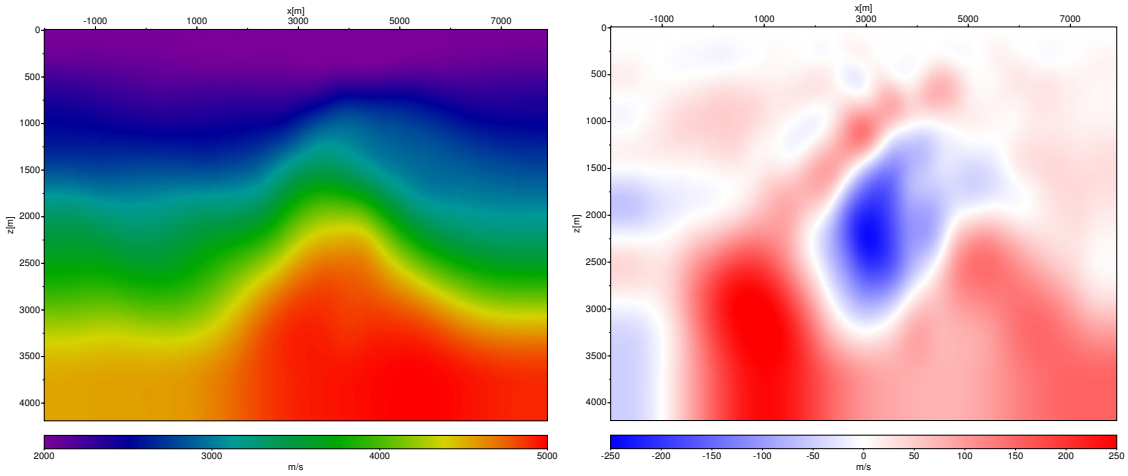

(a) Velocity model **(b)** Difference model

Figure 7: Left: velocity model obtained from NIP wave tomography with the corrected dataset. Right: velocity differences between the velocity models obtained with conventional and corrected datasets.

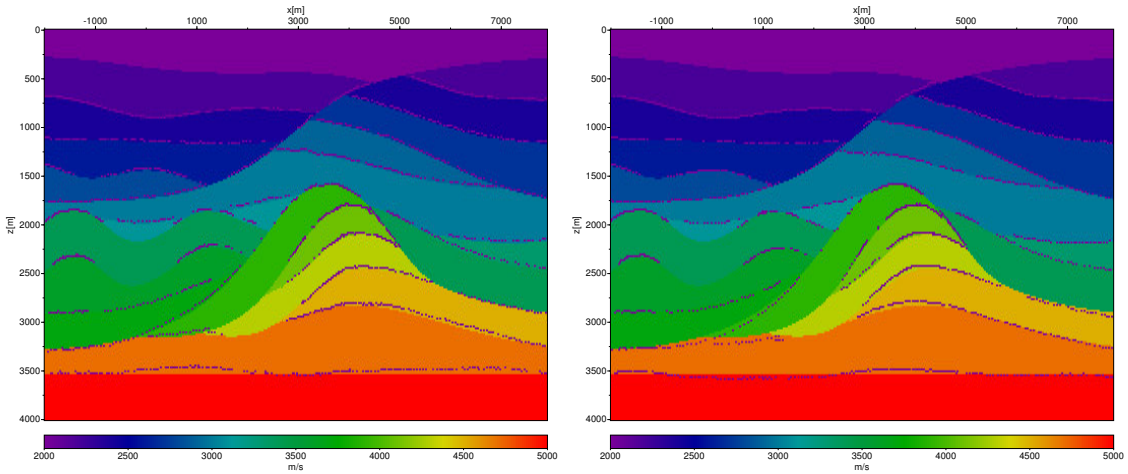

(a) Corrected dataset **(b)** Conventional dataset

Figure 8: Depth locations of the picks after tomography (left: with the corrected dataset, right: with conventional data).

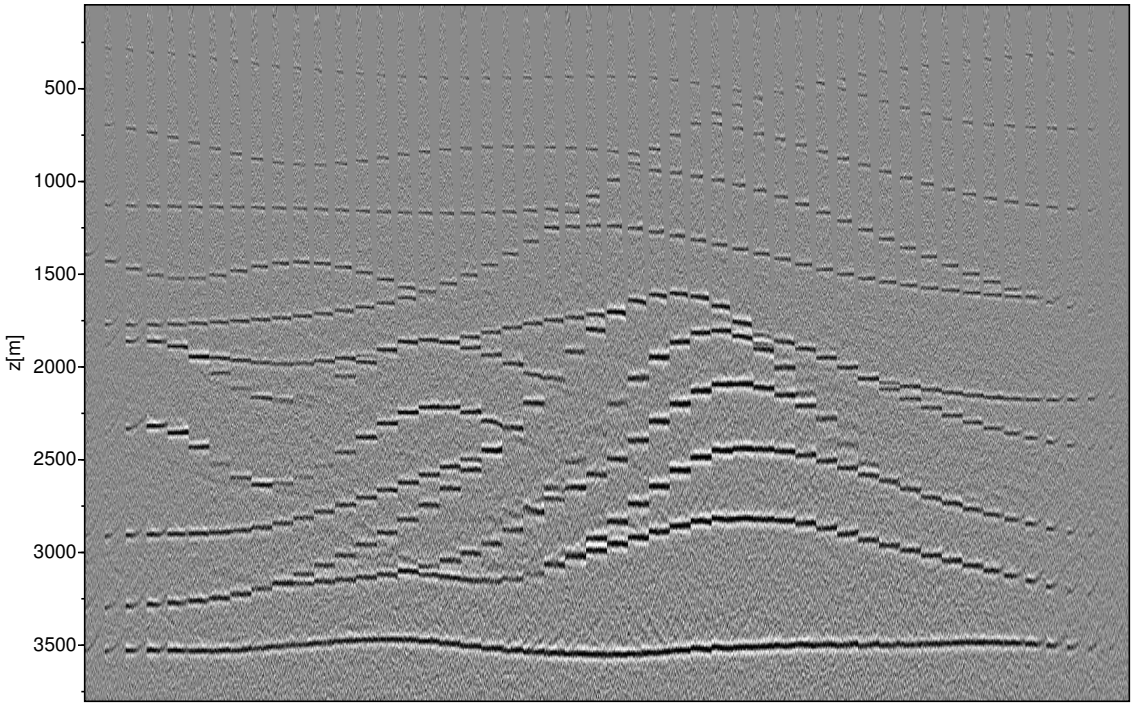

(a) Corrected dataset

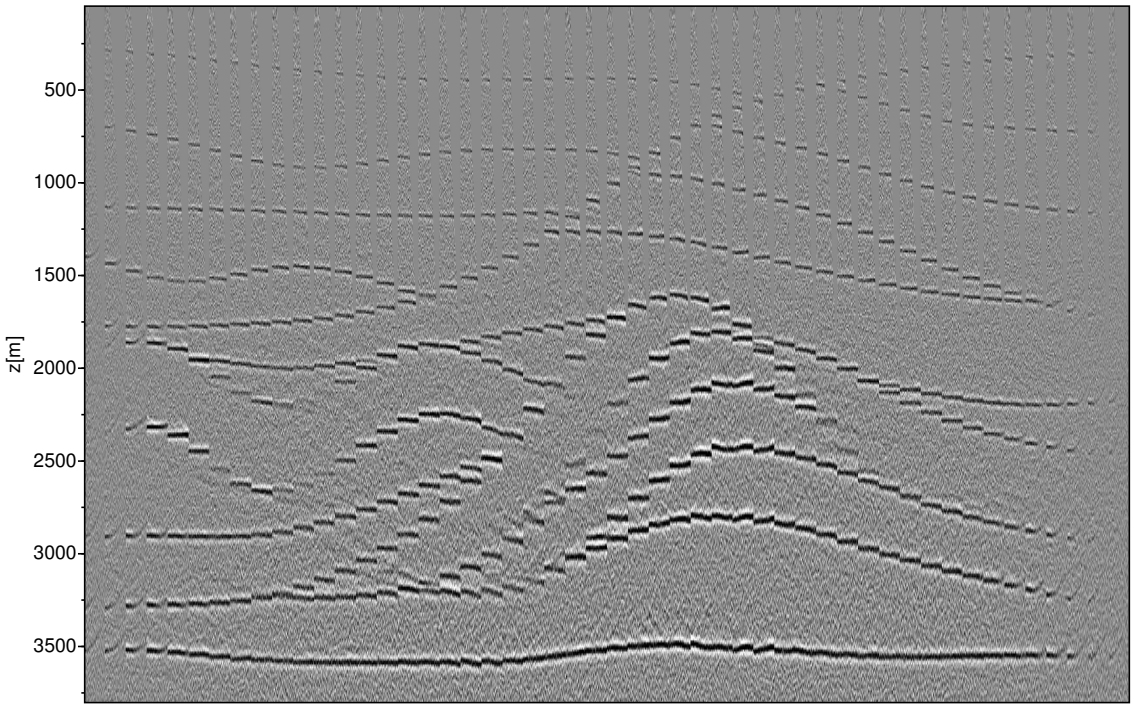

(b) Conventional dataset

Figure 9: Common-Image-Gathers after pre-stack depth migration (top: corrected attributes, bottom: conventional attributes).

describes the spread-length bias. The trajectories in the CMPA volumes defined by α_T allow to extract the "best fit" attributes related to reflection events. These attributes are then extrapolated to the correct quantities by means of a linear regression.

As shown for a synthetic data example, the corrected traveltimes and attributes provide better results in applications based on these quantities.

ACKNOWLEDGMENTS

This work was kindly supported by the sponsors of the *Wave Inversion Technology (WIT) Consortium*, Karlsruhe, Germany.

REFERENCES

Duveneck, E. (2004). Velocity model estimation with data-derived wavefront attributes. *Geophysics*, 69(1):265–274.

Höcht, G., de Bazelaire, E., Mayer, P., and Hubral, P. (1999). Seismics and optics: hyperbolae and curvatures. *J. Appl. Geoph.*, (42).

Hubral, P. and Krey, T. (1980). *Interval velocities from seismic reflection traveltime measurements*. Soc. Expl. Geophys.

Mann, J. (2002). *Extensions and applications of the Common-Reflection-Surface stack method*. Logos Verlag, Berlin.

Shah, P. M. and Levin, F. K. (1973). Gross properties of time-distance curves. *Geophysics*, 38(4):643–656.